

An extended formula of site-site Smoluchowski-Vlasov equation for electrolyte solution and infinitely dilute solution

Kenji Iida and Hirofumi Sato

Citation: *The Journal of Chemical Physics* **137**, 034506 (2012); doi: 10.1063/1.4732760

View online: <http://dx.doi.org/10.1063/1.4732760>

View Table of Contents: <http://scitation.aip.org/content/aip/journal/jcp/137/3?ver=pdfcov>

Published by the [AIP Publishing](#)

Articles you may be interested in

[Treatment of charged solutes in three-dimensional integral equation theory](#)

J. Chem. Phys. **128**, 134505 (2008); 10.1063/1.2841967

[Dielectric relaxation of electrolyte solutions using terahertz transmission spectroscopy](#)

J. Chem. Phys. **116**, 8469 (2002); 10.1063/1.1468888

[Submillimeter spectroscopic study of concentrated electrolyte solutions as high density plasma](#)

J. Chem. Phys. **116**, 5701 (2002); 10.1063/1.1458930

[Solvation in high-temperature electrolyte solutions. III. Integral equation calculations and interpretation of experimental data](#)

J. Chem. Phys. **114**, 3575 (2001); 10.1063/1.1343875

[Model representation of electrolyte solutions based on mass spectrographical data](#)

J. Chem. Phys. **109**, 4938 (1998); 10.1063/1.477105



Re-register for Table of Content Alerts

Create a profile.



Sign up today!



An extended formula of site-site Smoluchowski-Vlasov equation for electrolyte solution and infinitely dilute solution

Kenji Iida and Hirofumi Sato^{a)}*Department of Molecular Engineering, Kyoto University, Kyoto 615-8510, Japan*

(Received 4 April 2012; accepted 19 June 2012; published online 18 July 2012)

Solvation dynamics is one of the central subjects in solution chemistry. Site-site Smoluchowski-Vlasov (SSSV) equation is a diffusion equation for molecular liquid to analytically calculate the van Hove time correlation function. However, the application has been limited to simple solvent system such as liquid water because of the difficulty in solving the equation. In this study, an extended treatment of SSSV equation is proposed, which is applicable to a wide range of solution systems including mixed solution, electrolyte solution, and infinitely dilute solution. The present treatment realizes computation of the dynamics in LiCl aqueous solution, NaCl aqueous solution, and infinitely dilute aqueous solution of Li⁺ and Cs⁺ at the molecular level. © 2012 American Institute of Physics. [<http://dx.doi.org/10.1063/1.4732760>]

I. INTRODUCTION

Solvation dynamics is one of the central subjects in solution chemistry. Dielectric relaxation measurement and nuclear magnetic resonance (NMR) spectroscopy are representative experimental methods to treat solvation dynamics.¹⁻³ Using these techniques, the dynamics such as orientational relaxation and diffusional motion of molecule in solution system have been extensively studied. Numerous experimental techniques including femtosecond dielectric relaxation spectroscopy, femtosecond time-resolved infrared spectroscopy, two-dimensional infrared spectroscopy, two-dimensional NMR spectroscopy, and so on⁴⁻¹³ are being developed to provide new findings.

Theoretical and computational methods provide various knowledge that is difficult to be accessed from experimental methods. One of the most popular approaches to study condensed phase is molecular dynamics (MD) simulation.¹⁴⁻²⁶ It is noted, however, that computation of an appropriate ensemble to understand dynamical property is generally difficult compared to static property. An alternative is analytical approach as typified by integral equation theory for molecular liquid. Reference interaction site model (RISM) (Refs. 27-30) is a representative theory to treat static property such as pair correlation function and solvation free energy, in which an ensemble of infinite numbers of solvent molecules can be treated. In other words, RISM equation is free from the so-called sampling problem and has been successfully applied to a variety of chemical phenomena.

Although the original RISM is a theory only for static property, an extended form of the equation enables us to treat solvation dynamics. Site-site Smoluchowski-Vlasov (SSSV) equation^{31,32} is basically a diffusion equation for molecular liquid, and provides van Hove correlation function describing solvation dynamics in an analytical manner.^{33,34} However, the application has been limited to simple pure liquids

such as water and methanol. This is because of the absence of general framework to solve SSSV equation, especially for solution system with complex composition. In particular, solvation dynamics in electrolyte solution system could not be treated in spite of its ubiquitousness.

In this study, we present an extended treatment of SSSV equation by utilizing the technique to calculate state transition matrix in control engineering. The formula is applicable to a variety of solution systems including electrolyte solution and infinitely dilute solution, which could not be treated in the original SSSV framework. An aqueous solution of LiCl is computed as the first application, and then an infinitely dilute aqueous solution of Li⁺ and Cs⁺ is investigated focusing on the dynamics of water molecule near Li⁺ and Cs⁺. An aqueous solution of NaCl is also investigated and compared with the result of MD simulation,²² which demonstrates the validity of the present treatment.

II. THEORY

A. SSSV equation

In SSSV equation, local density $\Delta\rho_\alpha(r, t)$ is employed as the dynamical variable

$$\Delta\rho_\alpha(r, t) = \left[\sum_a \delta(r - |\mathbf{r}_{\alpha a}(t)|) \right] - \rho_\alpha, \quad (1)$$

where $r = |\mathbf{r}|$, $\delta(\dots)$ is the delta function, $\mathbf{r}_{\alpha a}(t)$ is the position of site (atom) α of a th molecule at time t , and ρ_α is the mean number density of the species of α . SSSV equation³¹ describes the local density in the Fourier space (\mathbf{k}),

$$\Delta\rho_\alpha(k, t) = \int_{-\infty}^{\infty} e^{-i\mathbf{k}\cdot\mathbf{r}} \Delta\rho_\alpha(r, t) d\mathbf{r}, \quad (2)$$

as follows:

$$\frac{\partial}{\partial t} \Delta\rho(k, t) = -\mathbf{D} \cdot \boldsymbol{\rho} \cdot \boldsymbol{\Phi}(k) \cdot \Delta\rho(k, t), \quad (3)$$

^{a)} Author to whom correspondence should be addressed. Electronic mail: hirofumi@moleng.kyoto-u.ac.jp. FAX: +81-75-383-2799.

where k equals $|\mathbf{k}|$, \mathbf{D} and $\boldsymbol{\rho}$ are diagonal matrices

$$\mathbf{D} = \begin{pmatrix} D_1 & & \mathbf{0} \\ & \ddots & \\ \mathbf{0} & & D_m \end{pmatrix}, \quad \boldsymbol{\rho} = \begin{pmatrix} \rho_1 & & \mathbf{0} \\ & \ddots & \\ \mathbf{0} & & \rho_m \end{pmatrix}. \quad (4)$$

Here m is the number of sites constituting solvent, and D_α ($\alpha \in \{1, \dots, m\}$) is self-diffusion coefficient of α . $\Phi(k)$ in Eq. (3) is given as

$$\Phi(k) = k^2[\{\boldsymbol{\rho} \cdot \boldsymbol{\omega}(k)\}^{-1} - \mathbf{c}(k)], \quad (5)$$

where the element of $\mathbf{c}(k)$ and $\boldsymbol{\omega}(k)$ is the direct correlation function and intramolecular correlation function, respectively. Then the van Hove function is given as

$$\frac{\partial}{\partial t} \mathbf{G}(k, t) = -\mathbf{D} \cdot \boldsymbol{\rho} \cdot \Phi(k) \cdot \mathbf{G}(k, t), \quad (6)$$

where the element of $\mathbf{G}(k, t)$ is the van Hove function. The function in the real space between sites α and β , $G_{\alpha\beta}(r, t)$, is defined as

$$G_{\alpha\beta}(r, t) = \frac{1}{\rho_\beta} \langle \Delta\rho_\alpha(r, t) \Delta\rho_\beta(r=0, t=0) \rangle, \quad (7)$$

where $\langle \dots \rangle$ denotes the ensemble average. $\mathbf{G}(k, t=0)$ is then given as

$$\mathbf{G}(k, t=0) = \boldsymbol{\omega}(k) + \boldsymbol{\rho} \cdot \mathbf{h}(k), \quad (8)$$

where the matrix element of $\mathbf{h}(k)$ is the total correlation function. Equation (6) is rewritten using the inverse Laplace transform, \mathcal{L}^{-1} ,

$$\mathbf{G}(k, t) = \mathcal{L}^{-1}[\{s\mathbf{1} + \mathbf{D} \cdot \boldsymbol{\rho} \cdot \Phi(k)\}^{-1}] \cdot \mathbf{G}(k, t=0), \quad (9)$$

where $\mathbf{1}$ is unit matrix and s is the frequency corresponding to t .

If Eq. (9) is analytically solved, the van Hove function at an arbitrary time t is obtained. To obtain the inverse matrix in Eq. (9), the cofactor expansion has been employed.³² However, the elements of the inverse matrix obtained by the expansion become complex as the matrix size is increased. Accordingly, it becomes difficult to solve analytically the inverse Laplace transformation. This is the reason why the application of the equation has been limited to simple liquid sys-

tem consisting of a few numbers of sites such as H₂O and methanol.

B. Bulk solvent

In this study, a technique to calculate state transition matrix in control engineering is utilized. To generally solve Eq. (9) for bulk solvent system, diagonalization of $\mathbf{D} \cdot \boldsymbol{\rho} \cdot \Phi(k)$ is considered,

$$\mathbf{D} \cdot \boldsymbol{\rho} \cdot \Phi(k) = \mathbf{P}(k) \cdot \boldsymbol{\lambda}(k) \cdot \mathbf{P}^{-1}(k), \quad (10)$$

where $\boldsymbol{\lambda}(k)$ is diagonal matrix with a set of the eigenvalues λ_m , and $\mathbf{P}(k)$ is the matrix consisting of the corresponding eigenvectors. The inverse matrix of $s\mathbf{1} + \mathbf{D} \cdot \boldsymbol{\rho} \cdot \Phi(k)$ in Eq. (9) is then given as

$$\{s\mathbf{1} + \mathbf{D} \cdot \boldsymbol{\rho} \cdot \Phi(k)\}^{-1} = \mathbf{P}(k) \cdot (s\mathbf{1} + \boldsymbol{\lambda}(k))^{-1} \cdot \mathbf{P}^{-1}(k), \quad (11)$$

where the element of $(s\mathbf{1} + \boldsymbol{\lambda}(k))^{-1}$ is given as

$$\{(s\mathbf{1} + \boldsymbol{\lambda}(k))^{-1}\}_{\alpha\beta} = \begin{cases} \frac{1}{s + \lambda_\alpha(k)} & (\alpha = \beta), \\ 0 & (\alpha \neq \beta). \end{cases} \quad (12)$$

Using Eq. (11), the inverse Laplace transformation of Eq. (9) can be readily performed, then the following equation is obtained,

$$\mathbf{G}(k, t) = \mathbf{P}(k) \cdot \exp[-\boldsymbol{\lambda}(k)t] \cdot \mathbf{P}^{-1}(k) \cdot \mathbf{G}(k, t=0), \quad (13)$$

where $\exp[-\boldsymbol{\lambda}(k)t]$ is exponential matrix given as

$$\exp[-\boldsymbol{\lambda}(k)t] = \begin{pmatrix} \exp[-\lambda_1(k)t] & & \mathbf{0} \\ & \ddots & \\ \mathbf{0} & & \exp[-\lambda_m(k)t] \end{pmatrix}. \quad (14)$$

Here m is number of solvent sites. To derive Eq. (13), the following relationship of inverse Laplace transformation is utilized:

$$\mathcal{L}^{-1} \left[\frac{1}{s + \lambda_\alpha^V(k)} \right] = \exp[-\lambda_\alpha^V(k)t]. \quad (15)$$

Using Eq. (13), SSSV equation can be solved for an arbitrary solvent if the matrix $\mathbf{D} \cdot \boldsymbol{\rho} \cdot \Phi(k)$ is diagonalized. A problem is then how to diagonalize the matrix,

$$\mathbf{D} \cdot \boldsymbol{\rho} \cdot \Phi(k) = \begin{pmatrix} D_1 \rho_1 \Phi_{11}(k) & D_1 \rho_1 \Phi_{12}(k) & \cdots & D_1 \rho_1 \Phi_{1m}(k) \\ D_2 \rho_2 \Phi_{21}(k) & & & \\ \vdots & \ddots & & \vdots \\ D_m \rho_m \Phi_{m1}(k) & \cdots & & D_m \rho_m \Phi_{mm}(k) \end{pmatrix}. \quad (16)$$

While the diagonalization of Hermite matrix yields real eigenvalue and eigenvector, $\mathbf{D} \cdot \boldsymbol{\rho} \cdot \Phi(k)$ is not Hermitian except for the case of $\rho_1 = \rho_2 = \cdots = \rho_m$ and $D_1 = D_2$

$= \cdots = D_m$. In general, diagonalization of a non-Hermite matrix often yields complex eigenvalue and eigenvector. In the present case, however, by introducing a diagonal matrix \mathbf{C}

expressed as

$$\mathbf{C} = \begin{pmatrix} 1/\sqrt{D_1\rho_1} & & \mathbf{0} \\ & \ddots & \\ \mathbf{0} & & 1/\sqrt{D_m\rho_m} \end{pmatrix}, \quad (17)$$

Eq. (10) is rewritten as

$$\mathbf{C} \cdot \Phi(k) \cdot \mathbf{C}^{-1} = (\mathbf{C} \cdot \mathbf{P}(k)) \cdot \lambda(k) \cdot (\mathbf{C} \cdot \mathbf{P}(k))^{-1}. \quad (18)$$

Notice that this is an eigenvalue problem for $\mathbf{C} \cdot \Phi(k) \cdot \mathbf{C}^{-1}$ (the right-hand side of the equation). Because this matrix is evidently Hermite, its eigenvalues ($\lambda(k)$) and the corresponding eigenvectors, $\mathbf{C} \cdot \mathbf{P}(k)$, are real. Consequently, $\mathbf{P}(k)$ is real, too. In other words, Eq. (18) indicates that the diagonalization of matrix given by Eq. (16) yields real eigenvalues and eigenvectors. Hence, the diagonalization of matrix given by Eq. (16) always yields real eigenvalues and eigenvectors, which are physically appropriate as the solution of Eq. (13).

C. Solute–solvent system

In the case of infinitely dilute solution consisting of one solute molecule and solvent molecules, the number density

of solute (ρ^U) is infinitely small ($\rho^U \rightarrow 0$), where the superscript U denotes solute. If Eq. (17) is directly used, the corresponding element of \mathbf{C} diverges ($1/\sqrt{D_\alpha^U \rho_\alpha^U} \rightarrow \infty$). However, starting from Eq. (16), $s\mathbf{1} + \mathbf{D} \cdot \rho \cdot \Phi(k)$ for the infinitely dilute solution is given as

$$s\mathbf{1} + \mathbf{D} \cdot \rho \cdot \Phi(k) = \begin{pmatrix} s\mathbf{1} + k^2\mathbf{D}^U \cdot \omega^{U-1}(k) & \mathbf{0} \\ -k^2\mathbf{D}^V \cdot \rho^V \cdot \mathbf{c}^{VU}(k) & s\mathbf{1} + \mathbf{D}^V \cdot \rho^V \cdot \Phi^{VV}(k) \end{pmatrix}, \quad (19)$$

where V denotes solvent. The matrix element of $\mathbf{c}^{VU}(k)$ is the direct correlation function between solvent and solute. To solve Eq. (9) for the matrix given by Eq. (19), block diagonalization is considered,

$$k^2\mathbf{D}^U \cdot \omega^{U-1}(k) = \mathbf{P}^U(k) \cdot \lambda^U(k) \cdot \mathbf{P}^{U-1}(k),$$

$$\mathbf{D}^V \cdot \rho^V \cdot \Phi^{VV}(k) = \mathbf{P}^V(k) \cdot \lambda^V(k) \cdot \mathbf{P}^{V-1}(k). \quad (20)$$

Rewriting Eq. (19) with Eq. (20), the inverse matrix is given as

$$\{s\mathbf{1} + \mathbf{D} \cdot \rho \cdot \Phi(k)\}^{-1} = \begin{pmatrix} \mathbf{P}^U(k) \cdot (s\mathbf{1} + \lambda^U(k))^{-1} \cdot \mathbf{P}^{U-1}(k) & \mathbf{0} \\ -\mathbf{P}^V(k) \cdot (s\mathbf{1} + \lambda^V(k))^{-1} \cdot \mathbf{P}^{V-1}(k) & \\ \cdot k^2\mathbf{D}^V \cdot \rho^V \cdot \mathbf{c}^{VU}(k) & \mathbf{P}^V(k) \cdot (s\mathbf{1} + \lambda^V(k))^{-1} \cdot \mathbf{P}^{V-1}(k) \\ \cdot \mathbf{P}^U(k) \cdot (s\mathbf{1} + \lambda^U(k))^{-1} \cdot \mathbf{P}^{U-1}(k) & \end{pmatrix}. \quad (21)$$

Applying the Laplace transformation to Eq. (21), the following formula for $\mathbf{G}(k, t)$ is yielded (see Eq. (9)):

$$\mathbf{G}(k, t) = \begin{pmatrix} \mathbf{G}^{UU}(k, t) & \mathbf{G}^{UV}(k, t) \\ \mathbf{G}^{VU}(k, t) & \mathbf{G}^{VV}(k, t) \end{pmatrix}, \quad (22)$$

where the elements are given as

$$\mathbf{G}^{UU}(k, t) = \mathbf{P}^U(k) \cdot \exp[-\lambda^U(k)t] \cdot \mathbf{P}^{U-1}(k) \cdot \mathbf{G}^{UU}(k, t=0),$$

$$\mathbf{G}^{VU}(k, t) = \mathbf{P}^V(k) \cdot \mathbf{B}^{VU}(k) \cdot \mathbf{P}^{U-1}(k) \cdot \mathbf{G}^{UU}(k, t=0) + \mathbf{P}^V(k) \cdot \exp[-\lambda^V(k)t] \cdot \mathbf{P}^{V-1}(k) \cdot \mathbf{G}^{VU}(k, t=0),$$

$$\mathbf{G}^{UV}(k, t) = \mathbf{0},$$

$$\mathbf{G}^{VV}(k, t) = \mathbf{P}^V(k) \cdot \exp[-\lambda^V(k)t] \cdot \mathbf{P}^{V-1}(k) \cdot \mathbf{G}^{VV}(k, t=0). \quad (23)$$

The element of $\mathbf{B}^{VU}(k)$ in Eq. (23) is given as

$$B_{\alpha\beta}^{VU}(k) = \begin{cases} \frac{1}{\lambda_\alpha^V(k) - \lambda_\beta^U(k)} (\exp[-\lambda_\alpha^V(k)t] - \exp[-\lambda_\beta^U(k)t]) \{\mathbf{P}^{V-1}(k) \cdot (k^2\mathbf{D}^V \cdot \rho^V \cdot \mathbf{c}^{VU}(k)) \cdot \mathbf{P}^{U-1}(k)\}_{\alpha\beta} & (\lambda_\alpha^V(k) \neq \lambda_\beta^U(k)), \\ -t \exp[-\lambda_\alpha^V(k)t] \times \{\mathbf{P}^{V-1}(k) \cdot (k^2\mathbf{D}^V \cdot \rho^V \cdot \mathbf{c}^{VU}(k)) \cdot \mathbf{P}^{U-1}(k)\}_{\alpha\beta} & (\lambda_\alpha^V(k) = \lambda_\beta^U(k)), \end{cases} \quad (24)$$

where

$$\lim_{x \rightarrow 0} \frac{1}{x} (e^x - 1) = 1 \quad (25)$$

is used. $\mathbf{G}(k, t = 0)$ in Eq. (23) is given as

$$\begin{aligned} \mathbf{G}^{UU}(k, t = 0) &= \omega^U(k), \\ \mathbf{G}^{VU}(k, t = 0) &= \rho^V \cdot \mathbf{h}^{VU}(k), \\ \mathbf{G}^{UV}(k, t = 0) &= \mathbf{0}, \\ \mathbf{G}^{VV}(k, t = 0) &= \omega^V(k) + \rho^V \cdot \mathbf{h}^{VV}(k). \end{aligned} \quad (26)$$

Notice that the formula of $\mathbf{G}^{VV}(k, t)$ is the same as Eq. (13), which is derived in Sec. II B.

A few comments are made on $\mathbf{G}(k, t)$ in Eq. (23). $\mathbf{G}^{VU}(r, t)$ indicates the probability of finding a solvent molecule at r and t in the condition that a solute molecule is at $r = 0$ and $t = 0$. Hence, $\mathbf{G}^{VU}(r, t)$ and $\mathbf{G}^{VU}(k, t)$ are non-zero value. On the other hand, $\mathbf{G}^{UV}(r, t)$ and $\mathbf{G}^{UV}(k, t)$ are zero. This is because $\mathbf{G}^{UV}(r, t)$ corresponds to the probability of finding a solute molecule at r and t in the condition that a solvent molecule is at $r = 0$ and $t = 0$. Since the number of solute molecule is much smaller than that of solvent molecule, this probability is infinitely small, virtually zero. $\mathbf{G}^{UU}(k, t)$ of atomic molecule such as Li^+ and Cl^- is given as $G_{\alpha\alpha}^{UU}(k, t) = \exp[-k^2 D_\alpha t]$ from Eq. (23), which is the classical formula of the self-intermediate scattering function.³⁰ $G_{\alpha\alpha}^{UU}(k, t)$ of atomic molecule is therefore consistent with the experimental knowledge if the parameter D_α is taken from experimental data. It is also noted that Chong and Hirata proposed an *ab initio* theory for self-diffusion coefficient.^{35,36}

III. COMPUTATIONAL METHOD

LiCl aqueous solution of 0.01 mol L^{-1} is investigated as the first application of the present extended SSSV treatment. Infinitely dilute aqueous solutions of Li^+ and Cs^+ are then investigated focusing on the difference of water motion around these ions. NaCl aqueous solution of 1 mol L^{-1} is also investigated, and the result is compared with the MD simulation result.²² Calculations were carried out at 298.15 K. Lennard-Jones parameters and diffusion coefficients were taken from the literatures.^{37–45} These are shown in Table I.

In the following discussion $G_{\alpha\beta}(r, t)$ is mainly focused on. This function corresponds to the number density of site α at r on t in the condition that site β is at $r = 0$ and $t = 0$. The 2D contour map of $G_{\alpha\beta}(r, t)$ was plotted from $t = 0.0 \text{ s}$ to 5.0 ps at 0.1 ps intervals. Since $G_{\alpha\alpha}^{UU}(r, t = 0)$

TABLE I. Lennard-Jones parameters (σ , ϵ) and diffusion coefficients (D).

	σ (Å)	ϵ (kcal mol ⁻¹)	D (10 ⁻⁵ cm ² s ⁻¹)	
			Set A ^a	Set B ^a
Li	1.394	0.12800	1.029	...
Cs	6.057	0.00008	2.056	...
Na	2.274	0.10900	...	1.250
Cl	3.620	0.44800	2.032	1.770
O	3.166	0.15500	2.300	2.139
H	1.000	0.05600	2.300	2.139

^aThe parameter set B was used only for 1 mol L^{-1} NaCl system, which was set to be consistent with the previous experimental study.^{41–44} All other computations were performed with set A.^{41,45}

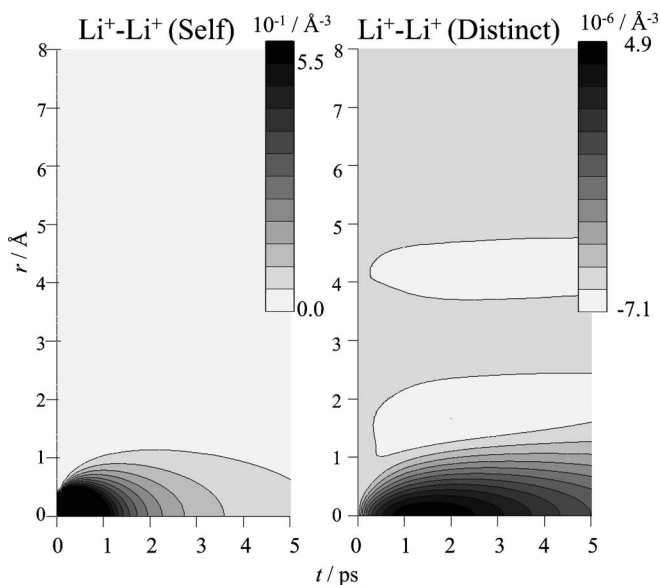


FIG. 1. The self-part of the correlation function of Li^+ ($G_{\text{Li}^+\text{Li}^+}^{UU}(r, t)$: left-hand panel), and the distinct part of the correlation function of Li^+ ($G_{\text{Li}^+\text{Li}^+}^{VU}(r, t)$: right-hand panel).

is the delta function, which cannot be numerically treated, $G_{\alpha\alpha}^{UU}(r, t = 0.01 \text{ ps})$ is alternatively employed to describe the area of $t < 0.1 \text{ ps}$.

IV. RESULT AND DISCUSSION

A. LiCl aqueous solution

The left panel of Figure 1 is the self-part of correlation function of Li^+ in LiCl aqueous solution, $G_{\text{Li}^+\text{Li}^+}^{UU}(r, t)$. This distribution means the probability density of finding Li^+ at r and t in the condition that the *same* Li^+ is at $r = 0 \text{ Å}$ and $t = 0 \text{ s}$. As the time proceeds, Li^+ diffuses from the initial position, $r = 0 \text{ Å}$, and the distribution becomes broader. Because the diffusion is spatially isotropic, the average position stays around $r = 0 \text{ Å}$. The right panel shows the distinct part between Li^+ (solvent) and Li^+ (solute). Note that $G_{\text{Li}^+\text{Li}^+}^{VU}(r, t)$ is simply plotted according to precedent while the number density is described by $G_{\text{Li}^+\text{Li}^+}^{VU}(r, t) + \rho_{\text{Li}^+}$. Because Li^+ at $r = 0 \text{ Å}$ and $t = 0 \text{ s}$ (solute) excludes other Li^+ (solvent), the distribution is not found at $r = 0 \text{ Å}$ and $t = 0 \text{ s}$. As time proceeds, the distribution at $r = 0 \text{ Å}$ increases and the peak is found at $t = 1.5 \text{ ps}$. As described below, Cl^- should exist near the origin. A plausible explanation of this peak is that Li^+ at $t = 0$ (solute) is replaced with other Li^+ (solvent) to make a different pair with the anion. Because solvent water molecules strongly coordinate to Li^+ , the replacement should occur between two solvation shells, respectively, consisting of Li^+ and water molecules. It is also noted that the time scale of this replacement is consistent with the diffusion constant.

Figure 2 shows the intermolecular correlation function between Cl^- and Li^+ , $G_{\text{Cl}^-\text{Li}^+}^{VU}(r, t)$. Similarly, $G_{\text{Cl}^-\text{Li}^+}^{VU}(r, t) + \rho_{\text{Cl}^-}$ corresponds to the number density of Cl^- in the condition that Li^+ is at $r = 0 \text{ Å}$ and $t = 0 \text{ s}$. The sharp peak at $r = 2 \text{ Å}$ and $t = 0 \text{ s}$ is evidently Cl^- adjacent to Li^+ . The peak height decreases and the width is broadened as the time

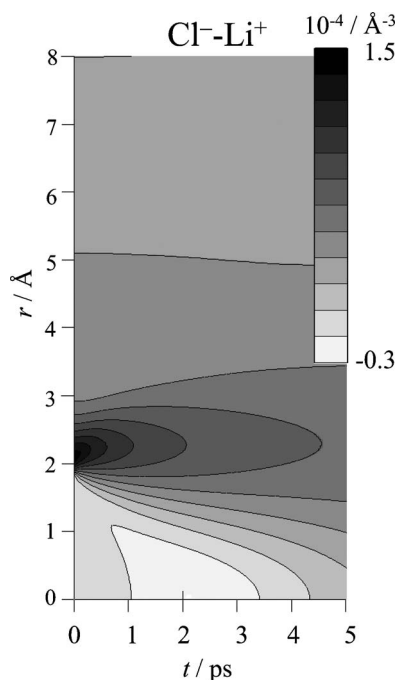


FIG. 2. Correlation function between Cl^- and Li^+ ($G_{\text{Cl}^- \text{Li}^+}^{\text{VU}}(r, t)$).

proceeds. According to the definition of the van Hove correlation function, this change is assigned to motion of Cl^- with respect to the position occupied by Li^+ at $t = 0$ s (the origin). Because Cl^- is strongly attracted by Li^+ , the decrease and broadening would be mainly attributed to accompanying Li^+ that moves from $r = 0$ Å. As illustrated in Figure 3, when Li^+ moves toward the Cl^- (i), Cl^- goes further, which contributes to the peak broadening to longer r . On the other hand, when Li^+ moves away from Cl^- (ii), the anion should also move to the same direction because of the strong interaction. This contributes to the broadening to shorter r . As discussed above, solvation shell of Li^+ may be exchanged with a different shell during this movement. A significant broadening of Cl^- occurs within ~ 3 ps, which is a similar time scale of Li^+ shell exchange. Consequently, Li^+ and Cl^- tend to make a pair because of the strong Coulombic interaction between them. However, this is dissolved within a few ps, which is mainly governed by diffusion process of ions.

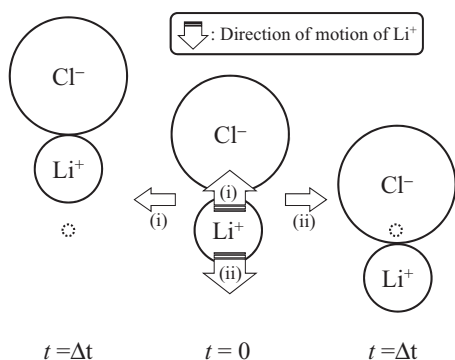


FIG. 3. Schematic motion of Cl^- adjacent to Li^+ . Dotted circle is the position of Li^+ at $t = 0$.

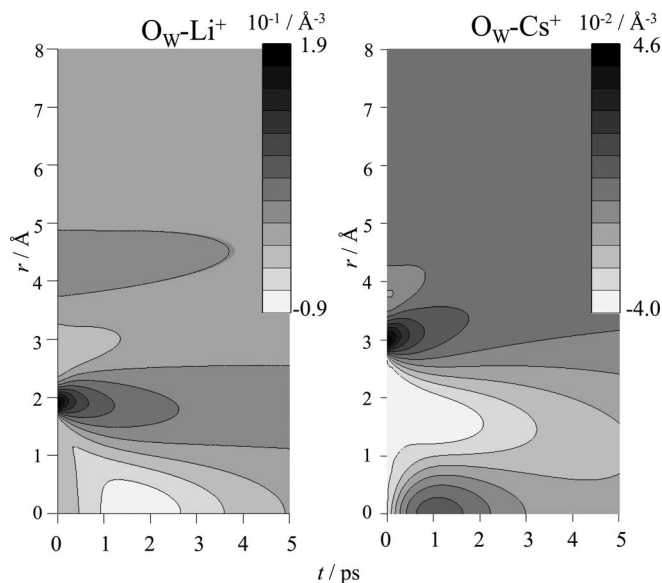


FIG. 4. Correlation function between O_w and Li^+ ($G_{\text{O}_w \text{Li}^+}^{\text{VU}}(r, t)$; left-hand panel), and correlation function between O_w and Cs^+ ($G_{\text{O}_w \text{Cs}^+}^{\text{VU}}(r, t)$; right-hand panel).

B. Water dynamics around Li^+ and Cs^+

Here we compare water motion around Li^+ and that around Cs^+ . Li^+ strongly attracts water whereas Cs^+ weakly attracts water comparing to Li^+ . Accordingly, the dynamics of water around these ions are different from each other.

The left panel of Figure 4 is the correlation function of water oxygen (O_w) around Li^+ , $G_{\text{O}_w \text{Li}^+}^{\text{VU}}(r, t)$. Since the peak at $r = 2$ Å and $t = 0$ s corresponds to the first solvation shell, the change of peak profile reflects the motion of O_w that is adjacent to Li^+ at $t = 0$ s. The peak position ($r \sim 2$ Å) remains unchanged, indicating the strong interaction between Li^+ and O_w . A water molecule is rarely separated from the ion. The right panel shows the correlation function of O_w around Cs^+ , $G_{\text{O}_w \text{Cs}^+}^{\text{VU}}(r, t)$. The peak at $r = 3$ Å and $t = 0$ s corresponds to the first solvation shell, and this peak position is in well accord with other studies ($r = 3.0\text{--}3.2$).^{46,47} The peak height (0.046) is much lower than that of the Li^+ case (0.19). This is, of course, attributed to the difference in the interaction strength between the two ions. The time evolution of the distribution is clearly different from the Li^+ case especially in terms of the peak position. Figure 5 plots the first peak position (r_{max}) of $G_{\text{O}_w \text{Li}^+}^{\text{VU}}(r, t)$ and $G_{\text{O}_w \text{Cs}^+}^{\text{VU}}(r, t)$ as a function of t . As noted above, the peak position of O_w around Li^+ remains mostly unchanged. On the other hand, the peak position of O_w around Cs^+ shifts away about 1 Å. The difference may be readily understood by looking at the distribution in the Cs^+ case at $r \sim 0$ Å and $t \sim 1.5$ ps. Because Cs^+ exists at the origin at $t = 0$ s, this distribution of O_w clearly indicates that Cs^+ moves from the original position and the generated vacant space is fulfilled with another water molecule to participate the hydration. The correlation function therefore implies that the solvation shell around Cs^+ is readily rearranged. Notice that the corresponding distribution at $r \sim 0$ Å is not found in the case of O_w around Li^+ . This is because the solvation

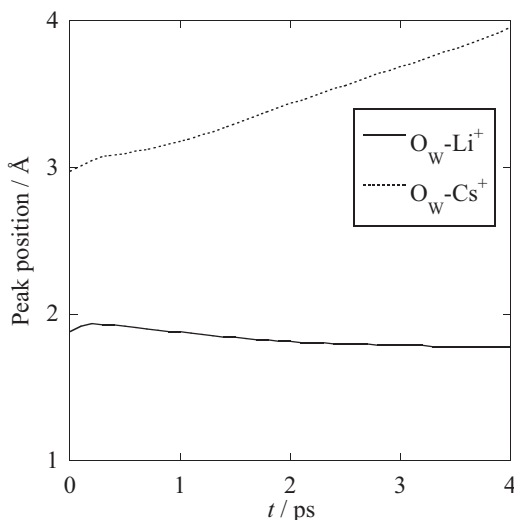


FIG. 5. Dependency of peak position (r_{\max}) on time t of the correlation function between O_w and Li^+ (solid line), and between O_w and Cs^+ (dashed line).

shell around Li^+ is more rigid than that around Cs^+ , as shown by the experimental studies.¹⁻³

Figure 6 shows the time evolution of correlation functions normalized with respect to the peak top,

$$G_{O_w Li^+}^{VU}(r = r_{\max}, t) / G_{O_w Li^+}^{VU}(r = r_{\max}, 0) \text{ and}$$

$$G_{O_w Cs^+}^{VU}(r = r_{\max}, t) / G_{O_w Cs^+}^{VU}(r = r_{\max}, 0).$$

The value of this function at $t = 0$ is one and converges to zero at $t = \infty$. Since the logarithmic axis is employed, a linear line corresponds to the ideal exponential decay. Clearly, the decay of the Li^+ case is slower than that of Cs^+ , indicating that the relative motion of water molecule around Li^+ is slower and the hydration structure is rigid compared to that around Cs^+ . While the hydration dynamics of Cs^+ is

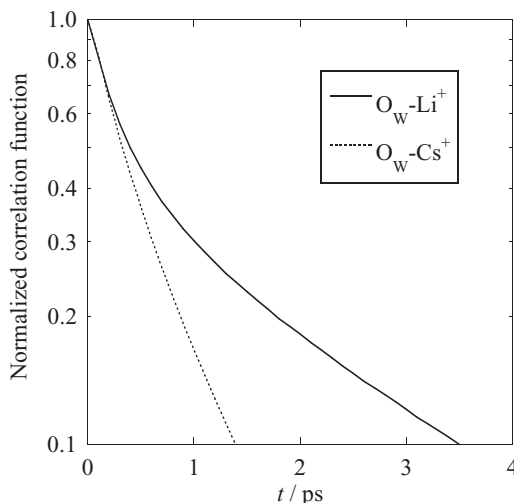


FIG. 6. Normalized correlation function in terms of peak top, $\ln\{G_{O_w Li^+}^{VU}(r = r_{\max}, t) / G_{O_w Li^+}^{VU}(r = r_{\max}, 0)\}$ (solid line) and $\ln\{G_{O_w Cs^+}^{VU}(r = r_{\max}, t) / G_{O_w Cs^+}^{VU}(r = r_{\max}, 0)\}$ (dashed line).

almost perfectly described with the exponential function, the Li^+ case evidently deviates and strong hydration is observed. Since the fast decay is remarkable only in the case of Li^+ , we consider that the fast decay is related to the response to the motion of adjacent ion. The slow one is considered to be related to the translation and collective relaxation. These assignments are consistent with the shift of the peak position. It is also noted that in the studies with MD simulation, analogous assignments are applied.^{22,23} The correlation time of the water molecule rotation is reported based on molecular simulation; 6.8 ps for 2.2 M LiI solution at 305 K (Ref. 24) and 2.9 ps for dilute Cs^+ .²⁵ Although these cannot be directly compared, they should be related to the present slow dynamics in Li^+ system.

C. NaCl aqueous solution

Finally, 1 mol L^{-1} NaCl aqueous solution is computed to confirm the validity of the present approach since the van Hove function of this system was reported with MD simulation.²² To the best of our knowledge, the work by Zatsky and Svishchev is the only example of the report of the van Hove function in the present system. The computed van Hove functions of O_w around Cl^- and around Na^+ with the present treatment (not shown) resemble those obtained by the MD simulation, which is the good indication of the validity of the treatment. To evaluate the difference more quantitatively, the ratio of the peak height

$$G_{O_w Na^+}^{VU}(r = r_{\max}, t) / G_{O_w Na^+}^{VU}(r = r_{\max}, 0) \text{ and}$$

$$G_{O_w Cl^-}^{VU}(r = r_{\max}, t) / G_{O_w Cl^-}^{VU}(r = r_{\max}, 0)$$

is focused on, and the correlation times are evaluated by the double exponential fitting: 0.26 ps and 1.13 ps are obtained for O_w around Na^+ , 0.53 ps and 1.66 ps for that around Cl^- . Zatsky and Svishchev reported several correlation times based on MD simulation,²³ but it is not straightforward to compare the result because of the difference in the definition of the correlation time and of the sampling uncertainty in simulation. It is noted, however, that the present results are in the same time region with their values; τ_T 's corresponding to the translational correlation time evaluated from van Hove functions in their work; 2.2 and 0.8 ps for Na^+ and 1.5 and 0.3 ps for Cl^- , respectively, evaluated at 298 and 378 K. Namely, strong temperature dependency was reported. They also reported the correlation time of rotation (τ_R , 1–5 ps), and the correlation time of the system derived from the dielectric properties (τ_1 , τ_2 , and τ_3), in which the fast component (τ_1) is independent on the temperature (~ 0.15 ps). Several rotational times of water ranging from 3 to 7 ps are also reported based on MD studies,²⁶ in which van Hove function was not evaluated. As a whole, the computed correlation time seems to be slightly faster than the other studies. Similar tendency was already pointed out by Nishiyama *et al.* on the studies of simple ion in acetonitrile solution. They showed that the decay rate obtained with the SSSV equation is faster than that with the mode-coupling theory.⁴⁸ Further careful investigation on the van Hove function is highly desired, both from molecular

simulation and from statistical mechanics. Anyway, it would be interesting that the present theory reasonably describes the solvation dynamics using only the diffusion constant.

V. CONCLUSION

In this study, a generalized treatment of SSSV equation was proposed. The obtained equation is applicable to a variety of solution including electrolyte solution and infinitely dilute solution. The van Hove correlation function of LiCl aqueous solution and infinitely dilute aqueous solution of Li⁺ and Cs⁺ were computed. The differences of water motion around Li⁺ and Cs⁺ were discussed focusing on the shift of peak position as well as the normalized correlation function.

NaCl solution was then computed to compare with the result of MD simulation. The obtained time constants show reasonably agree with the simulation results. It is also noted that in the case of bulk water, a good agreement between the functions computed by SSSV and those by MD has been already known,³¹ and the general picture of solvation dynamics computed from the present treatment agrees well with the results from experimental knowledge. It is therefore concluded that the dynamical aspects of the hydration structure around ions are successfully described with the present approach.

ACKNOWLEDGMENTS

The work is financially supported in part by Grant-in-Aid for Scientific Research on Priority Areas “Molecular Science for Supra Functional Systems” (477-22018016), Grant-in-Aid for Scientific Research on Innovative Areas “Molecular Science of Fluctuations” (2006-21107511), as well as by Grant-in-Aid for Scientific Research (C) (20550013). K.I. thanks the Grand-in Aid for JSPS Fellows. The Strategic Programs for Innovative Research (SPIRE), the Computational Materials Science Initiative (CMSI), and the Ministry of Education, Culture, Sports, Science and Technology (MEXT) Japan are also acknowledged. Theoretical computations were partly performed using Research Center for Computational Science, Okazaki, Japan.

¹Y. Marcus, *Chem. Rev.* **109**, 1346 (2009).

²R. Buchner and G. Heftner, *Phys. Chem. Chem. Phys.* **11**, 8984 (2009).

³H. Ohtaki and T. Radnai, *Chem. Rev.* **93**, 1157 (1993).

⁴A. W. Omta, M. F. Kropman, S. Woutersen, and H. J. Bakker, *J. Chem. Phys.* **119**, 12457 (2003).

⁵A. W. Omta, M. F. Kropman, S. Woutersen, and H. J. Bakker, *Science* **301**, 347 (2003).

⁶K. J. Tielrooij, N. Garcia-Araez, M. Bonn, and H. J. Bakker, *Science* **328**, 1006 (2010).

⁷M. F. Kropman and H. J. Bakker, *Science* **291**, 2118 (2001).

⁸S. Park and M. D. Fayer, *Proc. Natl. Acad. Sci. U.S.A.* **104**, 16731 (2007).

⁹H. J. Bakker, *Chem. Rev.* **108**, 1456 (2008).

¹⁰H. J. Bakker and J. L. Skinner, *Chem. Rev.* **110**, 1498 (2010).

¹¹K. Kwak, S. Park, and M. D. Fayer, *Proc. Natl. Acad. Sci. U.S.A.* **104**, 14221 (2007).

¹²J. Zheng, K. Kwak, J. Asbury, X. Chen, I. R. Piletic, and M. D. Fayer, *Science* **309**, 1338 (2005).

¹³A. G. Palmer, *Chem. Rev.* **104**, 3623 (2004).

¹⁴M. R. Harpham, N. E. Levinger, and B. M. Ladanyi, *J. Phys. Chem. B* **112**, 283 (2008).

¹⁵S. Roy, S. Banerjee, N. Biyani, B. Jana, and B. Bagchi, *J. Phys. Chem. B* **115**, 685 (2011).

¹⁶S. M. Urahata and M. C. C. Ribeiro, *J. Chem. Phys.* **124**, 074513 (2006).

¹⁷A. Heintz, R. Ludwig, and E. Schmidt, *Phys. Chem. Chem. Phys.* **13**, 3268 (2011).

¹⁸F. Brugué, M. Bernasconi, and M. Parrinello, *J. Am. Chem. Soc.* **121**, 10883 (1999).

¹⁹E. Kassab, E. M. Evleth, and Z. D. H-Tahra, *J. Am. Chem. Soc.* **112**, 103 (1990).

²⁰T.-M. Chang and L. X. Dang, *J. Chem. Phys.* **19**, 8813 (2003).

²¹D. Laage and J. T. Hynes, *Proc. Natl. Acad. Sci. U.S.A.* **104**, 11167 (2007).

²²A. Y. Zaslavsky and I. M. Svishchev, *J. Chem. Phys.* **115**, 1448 (2001).

²³I. M. Svishchev and A. Y. Zaslavsky, *J. Chem. Phys.* **112**, 1367 (2000).

²⁴G. I. Szász and K. Heinzinger, *J. Chem. Phys.* **79**, 3467 (1983).

²⁵C. F. Schwenk, T. S. Hofer, and B. M. Rode, *J. Phys. Chem. A* **108**, 1509 (2004).

²⁶S. Bouazizi and S. Nasr, *J. Mol. Liq.* **162**, 78 (2011); S. Chowdhuri and A. Chandra, *J. Chem. Phys.* **115**, 3732 (2001); J. Sala, E. Guàrdia, and J. Marti, *ibid.* **132**, 214505 (2010); A. Chandra, *J. Phys. Chem. B* **107**, 3899 (2003).

²⁷D. Chandler and H. C. Andersen, *J. Chem. Phys.* **57**, 1930 (1972).

²⁸F. Hirata and P. J. Rossky, *Chem. Phys. Lett.* **83**, 329 (1981).

²⁹*Molecular Theory of Solvation*, edited by F. Hirata (Kluwer, Dordrecht, The Netherlands, 2003).

³⁰J.-P. Hansen and I. R. McDonald, *Theory of Simple Liquids*, 3rd ed. (Academic, London, 2006).

³¹F. Hirata, *J. Chem. Phys.* **92**, 4619 (1992).

³²F. Hirata, T. Munakata, F. Raineri, and H. L. Friedman, *J. Mol. Liq.* **65/66**, 15 (1995).

³³L. Van Hove, *Phys. Rev.* **95**, 249 (1954).

³⁴H. L. Friedman, *A Course in Statistical Mechanics* (Prentice-Hall, Englewood Cliffs, NJ, 1985).

³⁵S.-H. Chong and F. Hirata, *Phys. Rev. E* **57**, 1691 (1998).

³⁶S.-H. Chong and F. Hirata, *Phys. Rev. E* **58**, 6188 (1998).

³⁷B. M. Pettitt and P. J. Rossky, *J. Chem. Phys.* **84**, 5836 (1986).

³⁸J. Åqvist, *J. Phys. Chem.* **94**, 8021 (1990).

³⁹M. Kinoshita and F. Hirata, *J. Chem. Phys.* **106**, 5202 (1997).

⁴⁰H. J. C. Berendsen, J. P. M. Postma, W. F. van Gunsteren, and J. Hermans, *Intermolecular Forces*, edited by B. Pullman (Reidel, Dordrecht, 1981).

⁴¹K. R. Harris and L. A. Woolf, *J. Chem. Soc., Faraday Trans.* **76**, 377 (1980).

⁴²D. W. McCall and D. C. Douglass, *J. Phys. Chem.* **69**, 2001 (1965).

⁴³J. H. Wang and S. Miller, *J. Am. Chem. Soc.* **74**, 1611 (1952).

⁴⁴J. H. Wang, *J. Am. Chem. Soc.* **74**, 1612 (1952).

⁴⁵*CRC Handbook of Chemistry and Physics*, 84th ed., edited by D. R. Lide (CRC, Boca Raton, FL, 2003).

⁴⁶K. P. Jensen and W. L. Jorgensen, *J. Chem. Theory Comput.* **2**, 1499 (2006).

⁴⁷Y. Marcus, *Chem. Rev.* **88**, 1475 (1988).

⁴⁸K. Nishiyama, T. Yamaguchi, F. Hirata, and T. Okada, *Pure Appl. Chem.* **76**, 71 (2004); *J. Solution Chem.* **33**, 631 (2004).